Pyrosol deposition of anatase TiO2 thin films starting from Ti(OiPr)4/acetylacetone solutions

Florin-Daniel Duminica, Francis Maury, S. Abisset

Pyrosol deposition of anatase TiO_2 thin films starting from $Ti(O^iPr)_4$/acetylacetone solutions

F.-D. Duminica [a], F. Maury [a,*], S. Abisset [b]

[a] *CIRIMAT, CNRS/INPT, ENSIACET, 118 Route de Narbonne, 31077 Toulouse cedex 4, France*
[b] *ARCELOR Atlantique et Lorraine, Route de Saint Leu, BP 30109, 60761 Montataire cedex, France*

Abstract

TiO_2 thin films were deposited on Si(100) and steel substrates by Pyrosol technique. The layer morphology depends on the concentration of titanium tetra-isopropoxide (TTIP) used as molecular precursor in solutions with acetylacetone (Acac). The concentration and, as a result, the viscosity of these TTIP/Acac starting solutions plays an important role on the efficiency of their nebulization and, consequently, on the microstructure and the growth kinetics of the TiO_2 thin films. The correlations between the composition of the TTIP/Acac solutions and the structure, the morphology, optical properties and the deposition rate of the films are presented and discussed. Growth rates as high as 1.8 μm/min are obtained using pure TTIP without Acac solvent. The photocatalytic activity of these Pyrosol TiO_2 thin films grown using TTIP with and without Acac solvent has been investigated and a negative effect of the solvent was found.

Keywords: TiO_2; Titanium oxide; Pyrosol; Aerosol assisted CVD; Thin films; Photocatalysis; Microstructure

1. Introduction

In the last decade the interest of titanium dioxide thin films has been increased because of their applications in various technical fields. TiO_2 is a well known and a very attractive material owing to its chemical stability, its bio-compatibility and remarkable electrical and optical properties. Indeed, it exhibits a high dielectric constant and resistivity, a high refractive index and good optical transparency over a wide spectral range. As a result, TiO_2 thin films find several applications as for instance electrical insulator and protective layers in electronic devices and antireflective layers for optical multilayer coatings [1,2]. TiO_2 films have also been considered as future candidates as dielectric in dynamic random access memory storage capacitors [3]. Furthermore anatase TiO_2 nanoparticles offer additional advantages such as a low cost and highly photoactive material which exhibits a suitable band gap (E_g=3.2 eV) compatible with the redox potential of the H_2O/OH couple (−2.8 eV). It is also a self regenerating and recyclable material. For these properties TiO_2 is a major candidate as active material in new devices, including gas sensors [4,5], and photocatalyst used for the decontamination and purification of environmental pollutants [6,7].

Titanium oxide films have been deposited by several techniques using different titanium source materials, such as anodization [8], electrodeposition [9], sol–gel techniques [10,11], activated reactive evaporation [12], reactive dc magnetron sputtering [13], chemical vapor deposition (CVD) [14–16], chemical vapor infiltration [17], plasma enhanced chemical vapor deposition [18], electrostatic sol–spray deposition [19], spray pyrolysis deposition [20,21] and aerosol assisted CVD namely Pyrosol [22].

Pyrosol process consists of the transport, the vaporisation and the pyrolysis of an aerosol, *i.e.* a fine mist produced from a liquid solution using a pneumatic or a piezoelectric device. This technique has been used to deposit under atmospheric pressure conductive films of simple oxides such as ZnO, In_2O_3 and SnO_2, which are used for their electrical and optoelectrical properties [23,24] as well as multicomponent oxides such as

* Corresponding author. Tel.: +33 562 885 669; fax: +33 562 885 600.
E-mail address: francis.maury@ensiacet.fr (F. Maury).

doi:10.1016/j.tsf.2007.03.057

$LiNbO_3$ and $LiTaO_3$ for acoustic wave applications [25]. TiO_2 thin films were recently deposited on Si and quartz substrates by Pyrosol in the presence of oxygen using Ti-*n*-butoxide and Ti-diisopropoxide as molecular precursor diluted in isopropanol and ethanol, respectively [26–28]. These films exhibited a smooth surface morphology and a good crystallinity.

In this paper we report a study on the deposition under atmospheric pressure of TiO_2 thin films by Pyrosol technique using different starting solutions of titanium tetraisopropoxide (TTIP) in acetylacetone (Acac). We particularly focus on the influence of the Pyrosol process parameters and of the solution concentration on the growth rate and the microstructure of the films. Preliminary properties of these thin films are described and confirm their potential applications.

2. Experimental details

Pyrosol is related to the CVD process and is based on the transport, the vaporisation and the pyrolysis of an aerosol produced by ultrahigh frequency spraying of a solution. The liquid solution containing the reactants used as molecular precursor is placed in a glass vessel fitted at its bottom with a piezoelectric transducer. The volume of the solution in the vessel is automatically maintained constant using an additional container as previously described by Langlet and Joubert [29]. The transducer, excited near its own resonance frequency, produces at the surface of the solution a mist composed of ultrafine droplets, which are conveyed using an inert carrier gas, toward the deposition zone. The process operates under atmospheric pressure. N_2 was used as inert carrier gas with a fixed flow rate of 5 slm. No additional reactive gas such as oxidant gas was used in these experiments.

The success of the Pyrosol technique depends critically on the properties of the solution including the volatility and stability of the precursor. This last compound must be soluble in an adequate solvent and stable under the experimental conditions during its transport as an aerosol. Under these conditions the aerosol droplets vaporise at a certain distance from the heated substrate and the vapor undergoes near the substrate a thermal decomposition (CVD mode) leading to the growth of a thin film and production of gaseous by-products. A cold-wall vertical quartz reactor, 5 cm in diameter, was used for the deposition of the layers. Si(100) and steel substrates were placed on a stainless steel sample holder (3.2 cm in diameter) heated by high frequency induction. The surface of the substrate was perpendicular to the aerosol stream.

The structural characteristics of the films were studied by X-ray diffraction (XRD) using grazing and θ–θ geometry (Cu Kα) depending on the thickness of the films. The surface morphology and film thicknesses determined on cross sections were analyzed using a scanning electron microscope (LEO 435VP). The composition uniformity of the samples was analyzed by secondary ion mass spectrometry (SIMS) under Cs^+ sputtering. Photocatalytic activity was tested by analyzing the degradation of an Orange G aqueous solution irradiated under UV light using a high pressure mercury lamp with a main emission peak at 365 nm (Philips HPLN 125 W).

3. Results and discussion

3.1. Control of the aerosol

A first set of experiments were carried out to determine the flow rate of solution or the quantity of solution consumed to produce the aerosol under various Pyrosol conditions. This is directly related to the aerosol flow rate and then to the precursor flow rate when the concentration of the solution is known. We have examined the influence of various parameters including (i) the TTIP concentration in acetylacetone used as solvent, (ii) the power and (iii) the frequency used to produce the aerosol and (iv) the time of the experiment. The frequency was varied around the resonance frequency of our transducer, while the power was varied as fractions of the maximum power of our electronic generator. The frequency directly acts on the diameter of the droplets ejected from the surface of the liquid solution while the power influences the amount of droplets or, in other words, the aerosol flow rate. Table 1 presents the typical Pyrosol growth conditions for the deposition of TiO_2 films. The maximum power of the generator was 150 W, but the values used were adjusted to control the aerosol flow rate and they are given in percentage of the maximum power.

Special care is necessary to handle the solution because of the extreme reactivity of the TTIP to the moisture which can induce the formation of various mixed alkoxide/hydroxide compounds. For instance, in preliminary experiments without stringent precautions undesirable precipitates have been observed during the preparation and handling of the solution. Further, the different liquid solutions were prepared under the inert atmosphere of a glove box. The presence of acetylacetone as solvent reduces the chemical reactivity by steric hindrance and avoids partial hydrolysis and polycondensation of TTIP. As a result, clear, colorless and stable liquid solutions were prepared. Acetylacetone (Acac) exhibits favourable physical properties (viscosity, surface tension, density and volatility) to produce a good aerosol with high flow rate. For this reason this solvent is frequently chosen for film deposition by Pyrosol technique. Despite the capability of acetylacetone to be transported in large quantity in the form of an aerosol, the flow rate of the aerosol and further the growth rate of the films strongly depend on the concentration of the solution.

Two experimental procedures were used to determine the aerosol flow rate. When using TTIP/Acac solutions the volume of solution consumed during the run was measured before and after the nebulization. When pure TTIP was used without solvent the volume of consumed liquid was too low for a short period to be precisely determined. Alternatively the aerosol was trapped at the entrance of the reactor by bubbling through a

Table 1
Typical Pyrosol growth conditions

Concentration of TTIP/Acac solutions (mol/l)	Deposition temperature (K)	Total pressure (kPa)	Generator frequency (kHz)	Generator power (%)	Carrier gas flow rate (N_2) (slm)
0.5–3.5	673–973	100	800	25–55	5

water vessel. The resulting precipitate was dried and calcinated in air at 723 K during 5 h in order to obtain crystallized TiO_2 powder. Then, the amount of TTIP was calculated assuming the total transformation of TTIP in TiO_2.

The aerosol flow rate (F_a) depends on the vapor pressure (P), the viscosity (η) and surface tension (σ) of the solution as well as a coefficient K, which depends on the power used to generate the mist, according to [30]:

$$F_a = K\sqrt{\frac{P}{\eta\sigma}}. \quad (1)$$

As revealed by Eq. (1), the viscosity has an important role on the efficiency of the aerosol formation since the flow rate of the aerosol is inversely proportional to the square of the viscosity. Fig. 1 shows the variations of the viscosity and the flow rate of nebulized solutions as a function of the composition of the TTIP/Acac solution.

The volume of solution used to form the aerosol, *i.e.* the quantity of aerosol, significantly decreases by increasing the TTIP concentration. Above a concentration of 2 M of the TTIP/Acac solutions it was very difficult to form an aerosol. This is strongly correlated to changes in the viscosity of the solution which increases from 0.8 cP for diluted solution to 8.3 cP for 2 M and 2.5 M TTIP/Acac solutions. It is assumed that metal complexes like $Ti(i\text{-}OPr)_{4-x}(Acac)_x$ are formed in the solution for concentrations higher than the critical value 2 M. A lower value of viscosity (2.3 cP) is obtained for pure TTIP which makes possible its transport as an aerosol (pure TTIP without solvent corresponds to the 3.5 M solution). Whatever the generator power, there is a domain of frequency where the aerosol flow rate is maximum and nearly constant: it is named range of agreement frequency [31]. In our case this frequency was around 800 kHz and it was kept constant at this value for all series presented in this paper.

It was observed that the flow rate of solution consumed to generate the aerosol increases with the power before reaching a maximum which depends on the concentration. The curves are shifted toward the high values of the power when the concentration of TTIP/Acac solutions increases (Fig. 2). This is correlated to the increase of viscosity of TTIP/Acac solutions. As a result, the equivalent mole flow rate of TTIP can be controlled in a relatively large range, typically from $3.3 \cdot 10^{-4}$ mol/min (7.4 sccm) for a 0.5 M solution using a power of 35% to $9 \cdot 10^{-3}$ mol/min (201.6 sccm) for a 3.5 M solution (i.e. without solvent) using a power of 50%.

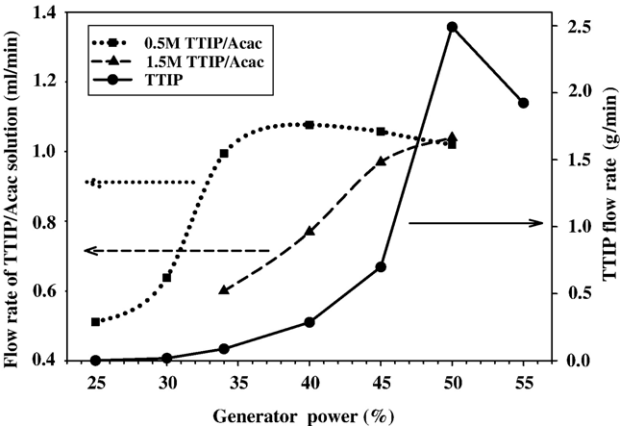

Fig. 2. Variation of the TTIP/Acac solution flow rate with the power used to produce the aerosol for various concentrations of the solutions.

The variation of the quantity of the solution consumed with the nebulization time is represented in Fig. 3. Using a 0.5 M TTIP/Acac solution we observe a linear increase, which indicates a constant aerosol flow rate (0.88 ml/min) over a period of about 40 min. For higher nebulization times a decrease of the aerosol flow is expected due to the preferential evaporation of solvent and so to the increase of concentration of TTIP/Acac solution in the vessel which was not thermostated.

3.2. Morphology and structure of the films

The coatings obtained by Pyrosol between 723 and 923 K using various TTIP/Acac solutions are single-phased and

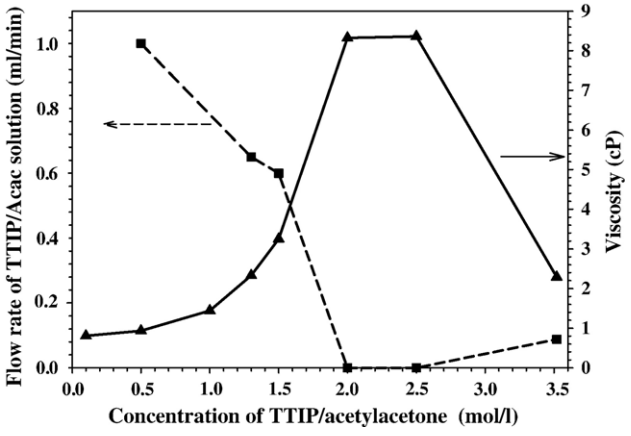

Fig. 1. Influence of the composition of TTIP/Acac solutions on the viscosity and the flow rate of liquid solution consumed during the Pyrosol runs using a power of 34% (all other parameters were kept constant).

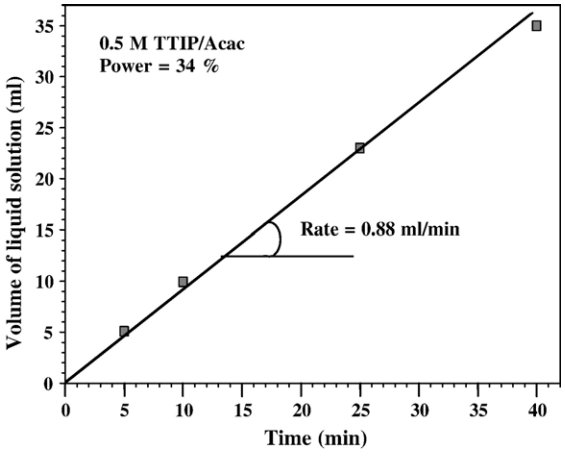

Fig. 3. Variation of the quantity of liquid solution consumed as a function of the nebulization time (carrier gas N_2=5 slm) using a 0.5 M TTIP/Acac diluted solution at room temperature and a power of 34%.

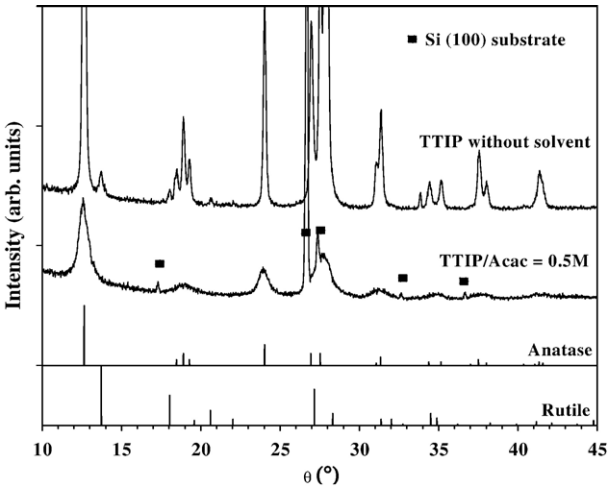

Fig. 4. XRD diffraction patterns (incidence angle 2°) of TiO_2 films synthesized by Pyrosol at 773 K using two starting solutions: 0.5 M TTIP/Acac and pure TTIP without solvent.

exhibit the anatase structure (Fig. 4). The crystallinity did not show major changes as a function of the deposition temperature in the explored range. Moreover, no significant effect of the substrate was found on the crystallinity. Typically the crystallite size estimated using the Scherrer formula is around 6 nm for films grown using diluted solutions. No significant change of crystallinity is observed for layers obtained starting from 0.5 M to 1.5 M TTIP/Acac solutions. No evidence for preferential orientation of the growth was found. Using TTIP/Acac diluted solutions, possibly the presence of Acac solvent molecules on the growing surface hinders the growth of large crystals of anatase leading to a nanocrystalline structure. A similar effect was reported for N-doped TiO_2 films [32].

The layers obtained using pure TTIP (without solvent) as starting solution consist of anatase/rutile mixtures whose ratio depends on the substrate temperature and the generator power. They exhibit a better crystallinity with a crystallite size larger than 30 nm. Under the explored conditions, the rutile amount is lower than anatase and it is favoured by the increase of the deposition temperature and by the decrease of the generator power, *i.e.* the TTIP mole fraction in the reactor, as already reported in conventional MOCVD process [33].

The films showed a good uniformity with different bright colors depending on their thickness. Due to the narrow distribution of the droplet size, the micro-droplets produced by ultrasonic pulverisation undergo a rapid vaporisation and pyrolysis leading to a homogeneously gas phase distribution on the substrate surface, which contributes to a good thickness uniformity of the films. A mapping of the thickness measured by SEM and reflectometry does not show great differences depending on the zone, indicating good thickness uniformity on substrates of a few square centimeters. The solvent seems to act as a surfactant during the deposition because when it is present a relatively high compactness of the film is observed. Using 0.5 M and 1.5 M TTIP/Acac diluted solutions, no morphological change was observed with the increase of the power. By contrast, using pure TTIP without solvent, we notice a variation of morphology by increasing the power (Fig. 5). So, for powers ranging from 30 to 45% the growth is columnar as already reported for CVD process using comparable TTIP mole fraction, whereas the layers are constituted of a mixture of micrometric and nanometric crystallites which form a compact structure using a power in the range 45–55% (the growth temperature was 773 K). As presented in Fig. 2, the amount of TTIP for the generator power range 45–55% is very high (TTIP mole fraction is around 3% in the gas phase). For temperatures in the range 723–773 K, the high concentration in the gas phase near the substrates leads to the formation of compact layers. For temperatures higher than 823 K, a homogeneous nucleation in the gas phase (powder formation) starts and a columnar growth is observed.

The morphology of the films changes by increasing the deposition temperature. The coatings obtained at 773 K from TTIP/Acac diluted solution are very compact and uniform. No

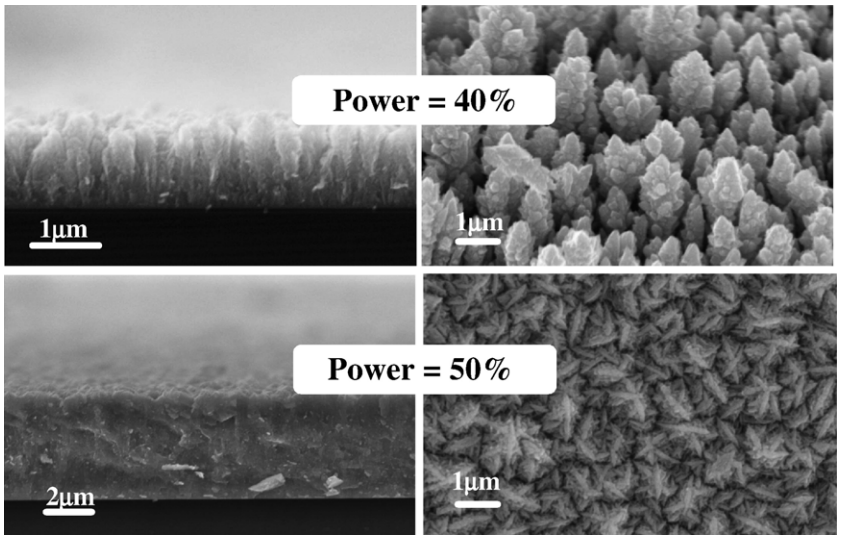

Fig. 5. SEM micrographs of surfaces and cross sections of two TiO_2 layers grown at 773 K using pure TTIP and two different powers to generate the aerosol (40 and 50%).

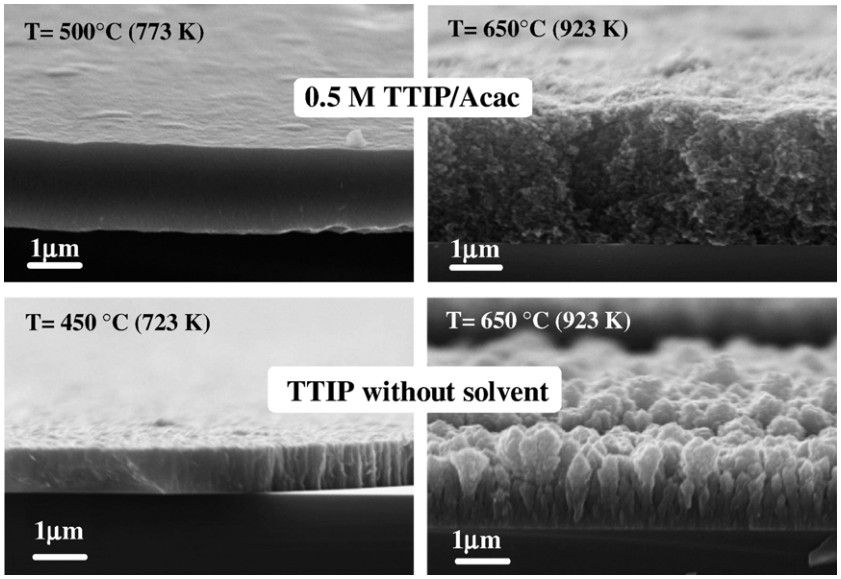

Fig. 6. SEM micrographs of cross sections of TiO_2 layers obtained from two starting solutions: 0.5 M TTIP/Acac at 773 and 923 K and pure TTIP at 723 and 923 K using a power of 34%.

grains are observed by SEM. Beyond 873 K the layers obtained using 0.5 M TTIP/Acac solution become porous and are constituted of nanometric grains (Fig. 6). Probably, the pyrolysis of the solvent that occurs at high temperature explains this morphological change. The coatings grown using TTIP without solvent exhibit also different morphologies when the deposition temperature increases. The growth is columnar over the whole temperature range (723–923 K) but the film porosity drastically increases with the temperature leading to a high specific surface area. This cauliflower-like structure was already observed for TiO_2 films grown by conventional MOCVD [33]. As a result, this Pyrosol process using diluted TTIP/Acac solutions and pure TTIP provides an easy way to deposit either compact and smooth films or layers exhibiting a high porous structure.

Fig. 7 shows reflectance spectra of two TiO_2 films (2500 nm) grown using 1.5 M TTIP/Acac solution and TTIP without solvent. The reflectance spectrum of the film grown starting from TTIP/Acac solution exhibits multiple oscillations in the visible and near infrared spectral range. This behavior is related to the high compactness of the films and gives good potentiality

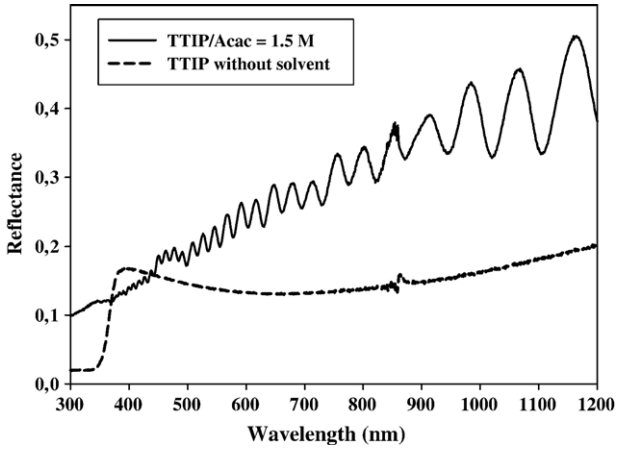

Fig. 7. Reflectance spectra of two TiO_2 films (2500 nm) grown at 773 K using 1.5 M TTIP/Acac solution and TTIP without solvent (power=40%). The oscillations when they are present were used to determine the film thickness.

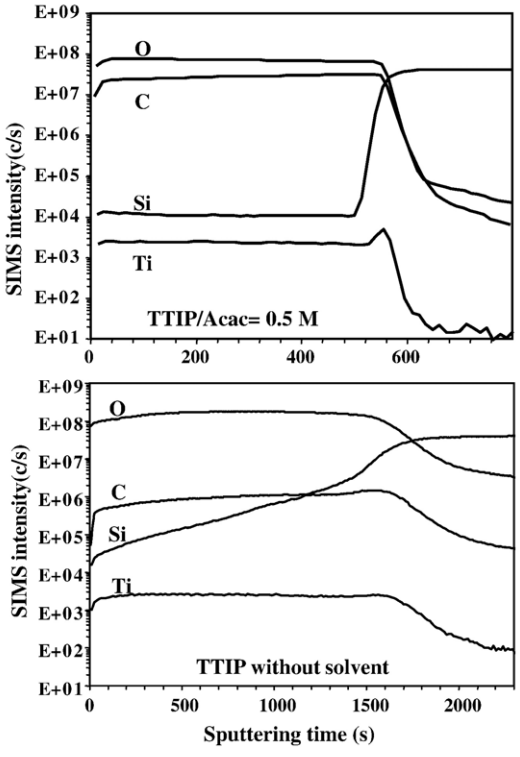

Fig. 8. SIMS depth profiles of two TiO_2 films grown using two starting solutions: 0.5 M TTIP/Acac and pure TTIP without solvent at 773 K using N_2 as carrier gas on Si substrate.

for optical applications. The refractive index measured by ellipsometry is typically 2.43 at 1.5 μm. The reflectance spectrum of the film grown starting from pure TTIP without solvent does not show such oscillations. This is due to the scattering of the light induced by the high porosity and the high surface roughness of this film. A higher absorption of the light in the 350–380 nm range is observed for the film grown starting from TTIP without solvent (band gap determined around 3.2 eV), while the film grown using TTIP/Acac solutions exhibits a higher reflectance in this wavelength range due probably to the highest amount of C incorporated in the film.

This assumption of C contamination is confirmed by the SIMS concentration profiles of two films obtained using 0.5 M TTIP/Acac and pure TTIP at 773 K, in both cases using a power of 34% (Fig. 8). The Ti and O profiles are flat and uniform. The Si profile originating from the substrate shows an abrupt interface for the layer grown using 0.5 M TTIP/Acac solutions in agreement with the highly compact structure of this film (Fig. 7). A relatively high concentration of carbon likely due to the decomposition of acetylacetone is found. This is in good agreement with the poor crystallinity of this film (Fig. 4). For the layer obtained using pure TTIP, the Si profile revealed an apparent diffuse interface. This is certainly due to the high porosity of the layer as revealed by Fig. 5. It is also noticed for this sample that the carbon contamination is significantly less important (almost two orders of magnitude lower) than in the layer obtained using TTIP/Acac solutions. This supports the assumption that the acetylacetone solvent significantly contributes to the carbon contamination of the Pyrosol TiO_2 layers.

3.3. Growth kinetics

The thickness of the TiO_2 films was found to increase linearly with the deposition time at 773 K for experiments carried out starting from a 0.5 M TTIP/Acac solution and using a power of 34%. This indicates a constant growth rate of 85 nm/min over several tens of minutes and permits a good reproducibility of the deposition process. Good thickness uniformity was also observed as evidenced by the homogeneous interferential colors of the samples.

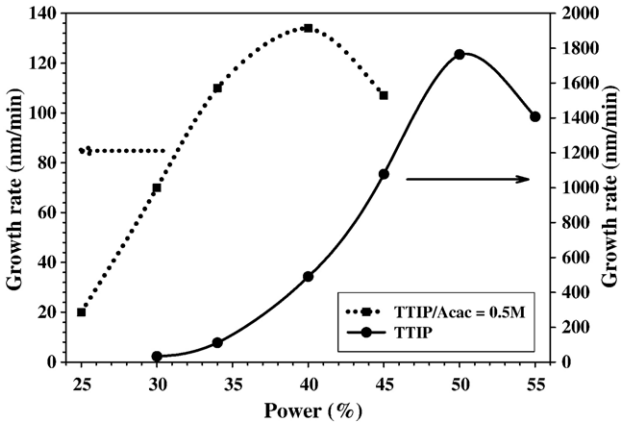

Fig. 10. Variation of the growth rate of TiO_2 Pyrosol films with the power used to generate the aerosol for two solutions: 0.5 M TTIP/Acac and pure TTIP without solvent.

Fig. 9 shows the variations of the growth rate with the deposition temperature for layers obtained using three solutions: 0.5 M TTIP/Acac, 1.5 M TTIP/Acac and pure TTIP using a power of 34% to generate the aerosol. The growth mode of the layers obtained from diluted TTIP/Acac solutions is kinetically controlled in the whole temperature range explored (723–923 K). For these diluted TTIP/Acac solutions, increasing the concentration of TTIP slightly decreases the deposition rate. This is probably due to the fact that by increasing the TTIP concentration the viscosity increases and, subsequently, the aerosol flow rate decreases as shown in Fig. 1. The apparent activation energy decreases from 174 kJ/mol to 135 kJ/mol by increasing the TTIP concentration from 0.5 M to 1.5 M. The variation of the growth rate with the temperature for the experiments carried out starting from pure TTIP reveals three kinetic modes: (i) a chemical kinetics regime at low temperature (723–823 K), (ii) probably a diffusion regime (823–873 K) and

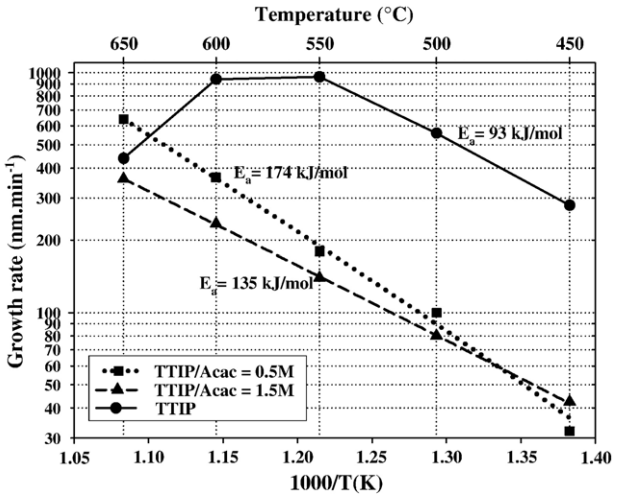

Fig. 9. Arrhenius plot of the growth rate of TiO_2 Pyrosol layers obtained from three solutions: 0.5 M TTIP/Acac, 1.5 M TTIP/Acac and pure TTIP without solvent (carrier gas N_2=5 slm, power=34%).

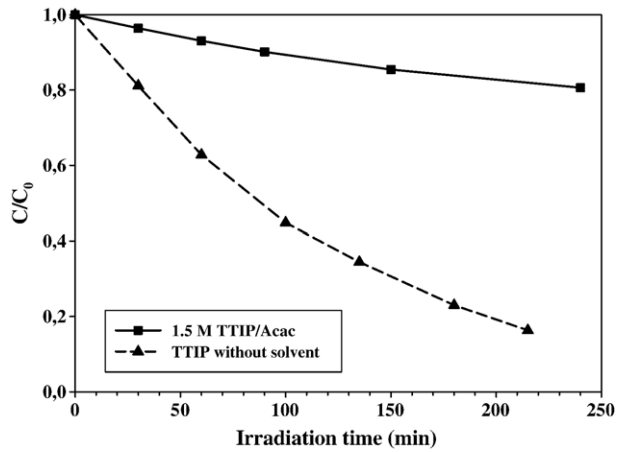

Fig. 11. Decomposition kinetics of an aqueous solution of Orange G (10 ppm) under UV light by two TiO_2 samples (2500 nm thick) grown on steel at 773 K using TTIP/Acac solution (1.5 M) and TTIP without solvent, respectively.

(iii) a depletion regime likely due to gas phase reactions occurring at high temperature (>873 K). This behavior is frequently found in conventional thermal CVD.

By increasing the power of the electronic generator, the quantity of liquid solution used to produce the aerosol, *i.e.* the aerosol flow rate, increases to reach a maximum before decreasing more or less rapidly depending on the concentration of the solution (Fig. 2). Fig. 10 shows the variation of the growth rate with the power of the electronic generator for Pyrosol runs carried out using a 0.5 M TTIP/Acac diluted solution and pure TTIP without solvent. The similarities between these curves and those reported on Fig. 2 clearly indicate a strong correlation between the aerosol flow rate and the growth of the TiO_2 thin films. The growth rate increases with the power to reach for instance 8 and 108 μm/h using 0.5 M TTIP/Acac solution and pure TTIP, respectively. This very high growth rate is noteworthy revealing that this Pyrosol process can be applied for a continuous deposition in a conveyor belt furnace.

4. Photocatalytic properties of Pyrosol TiO_2 films

When TiO_2 is exposed to UV light, it absorbs the photons whose energy is larger than the band gap and, subsequently, electrons–holes pairs are generated. The holes created in the valence band are transported toward the surface and react with water molecules producing hydroxyl radicals ($^{\cdot}OH$). The photo-generated electrons in the conduction band react with molecular oxygen (O_2) and produce superoxide (O_2^-) anion radicals [34]. These two reactive species oxidize readily the organic compounds adsorbed on the TiO_2 surface.

Fig. 11 shows the photocatalytic degradation of an aqueous solution of Orange G (10 ppm) by two TiO_2 samples (2500 nm thick) grown on steel substrate at 773 K using TTIP/Acac diluted solution (1.5 M) and TTIP without solvent, respectively. The sample was immersed into the Orange G solution chosen as model pollutant and irradiated under UV light. The sample grown using TTIP/Acac solution exhibit a low photocatalytic activity compared with the sample grown using pure TTIP without solvent. This last sample decomposes 50% of the initial quantity of orange G in approximately 75 min. The difference of photocatalytic activity is essentially explained by the difference in the specific surface area and the carbon contamination of the films. The sample grown using TTIP without solvent shows a higher specific surface area (Fig. 5) and a lower C contamination (less than 3 at.% by electron probe micro-analysis), while the sample grown using TTIP/Acac diluted solution shows a compact structure, a very smooth surface morphology (Fig. 6) and a higher C contamination (Fig. 8).

5. Conclusions

TiO_2 coatings were deposited by Pyrosol on various substrates. We have examined the influence of the TTIP concentration in acetylacetone, the power and the frequency used to produce the aerosol and the time of the deposition experiment. The viscosity of starting solutions plays an important role on the efficiency of nebulization of TTIP/Acac solutions and, consequently, on the microstructure and the growth rate of the TiO_2 thin films. Generally, different behaviors are found between the kinetic, morphological and structural features of the films grown using TTIP/Acac diluted solutions and pure TTIP without solvent. Their morphology, structure and purity can be controlled by changing the process parameters, specially the growth temperature and the TTIP/Acac concentration of the solutions. Single-phased (anatase) and bi-phased (anatase and rutile) coatings can be deposited at moderate temperature. Compact layers can be deposited using TTIP/Acac diluted solutions in the temperature range 673–823 K with interesting optical properties. Porous TiO_2 layers can be obtained using directly TTIP without solvent with promising photocatalytic activity. Both the high growth rate of Pyrosol TiO_2 films using TTIP without solvent and their good photocatalytic behavior under UV light make these films potentially interesting as supported photocatalysts for large scale applications. Further investigations on this process are currently in progress.

Acknowledgements

The authors would like to acknowledge ARCELOR for financial support and J. Dufour for technical assistance to set up the Pyrosol delivery system on a CVD reactor.

References

[1] C. Martinet, V. Paillard, A. Gagnaire, J. Joseph, J. Non-Cryst. Solids 216 (1997) 77.
[2] M.G. Kang, N.-G. Park, Y.J. Park, K.S. Ryu, S.H. Chang, Sol. Energy Mater. Sol. Cells 75 (2003) 475.
[3] S.A. Campbell, H.-S. Kim, D.C. Gilmer, B. He, T. Ma, W.L. Gladfelter, J. Res. Dev. 43 (1999) 383.
[4] M. Ferroni, V. Guidi, G. Martinelli, G. Faglia, P. Nelli, G. Sberveglieri, Nanostruct. Mater. 7 (1996) 709.
[5] M. Gerlich, S. Kornely, M. Fleischer, H. Meixner, R. Kassing, Sens. Actuators, B, Chem. 93 (2003) 503.
[6] I.K. Konstantinou, T.A. Albanis, Appl. Catal., B Environ. 42 (2003) 319.
[7] D. Robert, A. Piscopo, O. Heintz, J.V. Weber, Catal. Today 54 (1999) 291.
[8] J. Pouilleau, D. Devilliers, F. Garrido, S. Durand-Vidal, E. Mahe, Mater. Sci. Eng., B, Solid-State Mater. Adv. Technol. 47 (1997) 235.
[9] S. Karuppuchamy, K. Nonomura, T. Yoshida, T. Sugiura, H. Minoura, Solid State Ionics 151 (2002) 19.
[10] L. Zhang, Y. Zhu, Y. He, W. Li, H. Sun, Appl. Catal., B Environ. 40 (2003) 287.
[11] B. Li, X. Wang, M. Yan, L. Li, Mater. Chem. Phys. 78 (2003) 184.
[12] T. Fujii, N. Sakata, J. Takada, Y. Miura, Y. Daitoh, M. Takano, J. Mater. Res. 9 (1994) 1468.
[13] S. Takeda, S. Suzuki, H. Odaka, H. Hosono, Thin Solid Films 392 (2001) 338.
[14] V. Gauthier, S. Bourgeois, P. Sibillot, M. Maglione, M. Sacilotti, Thin Solid Films 340 (1999) 175.
[15] W. Li, S. Ismat Shah, C.-P. Huang, O. Jung, C. Ni, Mater. Sci. Eng., B, Solid-State Mater. Adv. Technol. 96 (2002) 247.
[16] B.-C. Kang, S.-B. Lee, J.-H. Boo, Surf. Coat. Technol. 131 (2000) 88.
[17] C. Sarantopoulos, F.-D. Duminica, A.N. Gleizes, F. Maury, in: R. Fischer (Ed.), Proceedings of the 15th European Conference on Chemical Vapor Deposition, The Electrochemical Soc. Proc., Pennington, NJ, 2005, p. 252.
[18] G.A. Battiston, R. Gerbasi, A. Gregori, M. Porchia, S. Cattarin, G.A. Rizzi, Thin Solid Films 371 (2000) 126.
[19] C.H. Chen, E.M. Kelder, J. Schoonman, Thin Solid Films 342 (1999) 35.

[20] M. Okuya, N.A. Prokudina, K. Mushika, S. Kaneko, J. Electrochem. Soc. 19 (1999) 903.
[21] L. Castaneda, J.C. Alonso, A. Ortiz, E. Andrade, J.M. Saniger, J.G. Banuelos, Mater. Chem. Phys. 77 (2002) 938.
[22] L. Kavan, M. Gratzel, Electrochim. Acta 40 (1995) 643.
[23] A. Smith, R. Rodriguez-Clemente, Thin Solid Films 345 (1999) 192.
[24] A. Smith, Thin Solid Films 376 (2000) 47.
[25] V. Bornand, I. Huet, P. Papet, E. Philippot, Ann. Chim. Sci. Matér. 26 (2001) 49.
[26] A. Conde-Gallardo, M. Guerrero, N. Castillo, A.B. Soto, R. Fragoso, J.G. Cabañas-Moreno, Thin Solid Films 473 (2005) 68.
[27] L. Cstañeda, J.C. Alonso, A. Ortiz, E. Andrade, J.M. Saniger, J.G. Bañuelos, Mater. Chem. Phys. 77 (2002) 938.
[28] A. Conde-Gallardo, N. Castillo, M. Guerrero, J. Appl. Phys. 98 (2005) 054908.
[29] M. Langlet, J.C. Joubert, in: C.N.R. Rao (Ed.), Chemistry in Adv. Mater. Blackwell Sci. Pub., Oxford, 1992, p. 55.
[30] E.L. Gershenzon, O.K. Eknadiosyants, Sov. Phys. Acoust. 10 (1964) 127.
[31] M. Mayne, N. Allain, X. Armand, N. Herlin-Boime, M. Cauchetier, 15ème Congrès Français sur les aérosols (CFA 99), Paris, Association Française d'Etudes et de Recherche sur les Aérosols, 1999, p. 107.
[32] J. Guillot, F. Fabreguette, L. Imhoff, O. Heintz, M.C. Marco de Lucas, M. Sacilotti, B. Domenichini, S. Bourgeois, Appl. Surf. Sci. 177 (2001) 268.
[33] F.-D. Duminica, F. Maury, F. Senocq, Surf. Coat. Technol. 188–189 (2004) 255.
[34] A. Mills, S. Le Hunte, J. Photochem. Photobiol., A Chem. 108 (1997) 1.